ELSEVIER
International Journal of Mass Spectrometry 218 (2002) 19–35
International Journal of Mass Spectrometry
www.elsevier.com/locate/ijms

# Theoretical studies on the isomerization and dissociation of the acrolein ions

Yue Li, Tomas Baer*

*Department of Chemistry, University of North Carolina, Chapel Hill, NC 27599-3290, USA*

Received 11 January 2002; accepted 28 March 2002

---

## Abstract

Nine isomers of the acrolein ion ($C_3H_4O^{\bullet+}$) and the relevant transition states connecting them were calculated at HF/6-31G* and B3LYP/6-31G* levels. The nine dissociation channels, $C_2H_4^{\bullet+}$ (+CO), $C_3H_3O^+$ (+H$^\bullet$), $HCO^+$ (+$C_2H_3^\bullet$), $H_2CO^{\bullet+}$ (+$C_2H_2$), $C_2H_3^+$ (+HCO$^\bullet$), $HCOH^{\bullet+}$ (+$C_2H_2$), $C_2H_2^{\bullet+}$ (+$H_2CO$), $CO^{\bullet+}$ (+$C_2H_4$), and $C_2H_2^{\bullet+}$ (+HCOH), were studied and the transition states to all product channels were found. The lowest energy dissociation path to CO loss involves a distonic ion, $^\bullet CH_2CH_2CO^+$, and the methylketene ion, $CH_3CHCO^{\bullet+}$ the latter being the most stable $C_3H_4O^{\bullet+}$ isomer. The heats of formation of the $C_3H_4O^{\bullet+}$ isomers are obtained based on the known heats of formation of $C_2H_4^{\bullet+}$ and CO and the calculated relative energies. (Int J Mass Spectrom 218 (2002) 19–35) © 2002 Elsevier Science B.V. All rights reserved.

*Keywords:* Acrolein; DFT calculations; Dissociation; Thermochemistry; Isomerization

---

## 1. Introduction

The acrolein molecule, $CH_2CHCHO$ (**1**), is one of the simplest multi-functional molecules (alkene and aldehyde). In addition, the molecule is a prototypical conjugated double bond system with interesting spectroscopic properties [1,2]; thus, it has received considerable attention, both experimentally [3–5] and theoretically [6,7]. However, no direct measurement of its heat of formation has been reported, and its estimates have differed significantly from theoretical results [8]. Similarly, the experimental heat of formation of the methylketene ion, an isomer of acrolein, has only recently been measured [9]. Thus, most of the energetic information about the $C_3H_4O$ and $C_3H_4O^{\bullet+}$ species has come from theoretical calculations.

Kikichi and coworkers [10] calculated the structures and energies of the *cis–trans* conformers of the acrolein molecule and ion and found that for both, the *trans*-conformer is more stable than the *cis*-conformer. In a 1987 theoretical study, Bouchoux [11] reported on 13 $C_3H_4O^{\bullet+}$ isomers including the acrolein ion at the UHF/6-31G(d,p)//3-21G level. This study revealed two structures with energies below that of the acrolein ion. They are a distonic ion, $^\bullet CH_2CH_2CO^+$ (**2**$^+$) calculated to be 34 kJ/mol more stable than the acrolein ion (**1**$^+$), and the methylketene ion, $CH_3CHCO^{\bullet+}$ (**3**$^+$), which is some 64 kJ/mol more stable than **1**$^+$. Traeger et al. [12] reported Hartree–Fock (HF) calculations with structures optimized using the 6-31G basis set, which showed that the **3**$^+$ energy is 35.7 kJ/mol lower than that of **2**$^+$, a result that agrees quite well with the 30 kJ/mol of Bouchoux [11]. However, in the higher theory level calculations (MP4) by

---

* Corresponding author. E-mail: baer@unc.edu

*PII* S1387-3806(02)00645-0

Turecek et al. [13,14], $\mathbf{2}^+$ is 85.6 kJ/mol lower than $\mathbf{1}^+$. So far, the highest level calculations were performed by McKee and Radom [8], who obtained the relative energies and heats of formation of the acrolein isomers including the neutral and ionic species using the G2 technique. In contrast to the results of Bouchoux [11], but in closer agreement with the MP4 results [13,14], they found that $\mathbf{2}^+$ is more stable than $\mathbf{1}^+$ by 73 kJ/mol, and that $\mathbf{3}^+$ is more stable than $\mathbf{1}^+$ by 119 kJ/mol.

Although the heats of formation of the neutral species have not been directly determined, several groups have measured the photoelectron spectrum of acrolein and determined an adiabatic ionization energy (IE) of 10.11 eV [15–19]. The heat of formation of the methylketene ion was recently reported by Traeger [9]. The photoionization onset of the ketene structure ($CH_3CHCO^{\bullet+}$) was measured for several precursor ions, including cyclopentanone, 3-pentanone, and 2-methyl-3-pentanone. These onsets resulted in a 298 K methylketene ion heat of formation of 783.5 kJ/mol. Because methylketene is a highly unstable molecule, only one experimental IE value has been reported [20]. Although a stable molecule, acrolein has not been studied by photoionization mass spectrometry so that the only information about the dissociation paths comes from electron ionization. The early electron ionization studies [21–23] reported only the production of two ions, *m*/*z* 29 ($HCO^+$) and *m*/*z* 27 ($C_2H_3{}^+$), which correspond to the direct dissociation of the acrolein ion by cleavage of the C–C single bond. However, Turecek et al. [13,14] studying the formation, isomerization and dissociation of several $C_3H_4O^{\bullet+}$ isomers by neutralization–reionization mass spectrometry (NRMS), found a much richer assortment of product ions. The acrolein, distonic, and methylketene ions all dissociated to $C_3H_3O^+ + H^\bullet$, $C_2H_4{}^{\bullet+} + CO$, $C_2H_3^+ + HCO^\bullet$, and $C_2H_2{}^{\bullet+} + H_2CO$.

Traeger et al. [12] studied the dissociation of $\mathbf{1}^+$, $\mathbf{2}^+$, and $\mathbf{3}^+$ by collisionally activated dissociation (CAD) spectrometry and found that all three isomers reacted via metastable decomposition by $H^\bullet$ or CO loss. On the basis of the translational energies released, they suggested that the distonic ion, $\mathbf{2}^+$, did not isomerize to the other ions prior to decomposition. The mechanism for the acrolein and methylketene ion decomposition, however, remained ambiguous in that the extent to which all three isomers rearrange during the dissociation is not clear.

The dissociation of the acrolein ion to $C_2H_4{}^{\bullet+}$, $CO^{\bullet+}$ or $C_2H_2{}^{\bullet+}$ clearly requires rearrangements prior to dissociation. However, no detailed experimental or theoretical investigation on the mechanisms and relevant energy barrier heights of these rearrangement reactions has been reported. The only result is that of McKee and Radom [8] who obtained the transition state that connects $\mathbf{3}^+$ and $\mathbf{2}^+$. In this study, we report on nine $C_3H_4O^{\bullet+}$ isomers and the transition states connecting them. These have been calculated in order to determine nine low-energy dissociation channels of the acrolein ion. In addition to these calculations, we have carried out photoelectron photoion coincidence (TPEPICO) spectroscopy experiments to investigate the dissociation dynamics of the acrolein ion. The experimental results, analyzed with the aid of the present calculations, are described in the accompanying paper.

## 2. Quantum chemical calculations

The calculations were performed on an Origin 2000 computer at UNC-Chapel Hill using the Gaussian-98 package [24]. All neutral and ionic species were fully optimized at the HF and DFT (B3LYP) levels using the 6-31G* basis set. The stationary points and first-order saddle points were confirmed through the calculation of harmonic vibrational frequencies, which were also used to obtain the zero point vibrational energies (ZPE). To obtain more reliable energy results, the single point calculations were performed at the B3LYP/6-311+G** level using the B3LYP/6-31G* equilibrium geometries. The transition states were obtained using the synchronous transit-guided quasi-Newton (STQN) methods [25,26]. In the B3LYP calculations for all open shell species, the spin-squared expectation values ($\langle S^2\rangle$) are close to 0.75, an ideal value for pure spin eigenstates so that the spin contaminations can be ignored. For all transition states, intrinsic reaction coordinate (IRC) calculations were performed to determine the isomers or dissociation channels to which the transition states evolved.

## 3. Results and discussion

### 3.1. Structures of the $C_3H_4O^{\bullet+}$ isomers and transition states

The equilibrium structures for neutral acrolein, nine of the $C_3H_4O^{\bullet+}$ isomers and the transition states along with some of the important bond distances and bond angles obtained at the B3LYP/6-31G* level are shown in Fig. 1. The bond lengths in this figure are in Ångstroms and the bond angles are in degrees. All of the isomers are obtained with only hydrogen atom transfer steps, leaving the C–C–C–O backbone intact. The energies in atomic units, $\langle S^2 \rangle$, zero point energies and relative energies for three levels of theory are listed in Table 1.

A comparison of the relative energies shows that the SP with the higher level basis set agrees very well

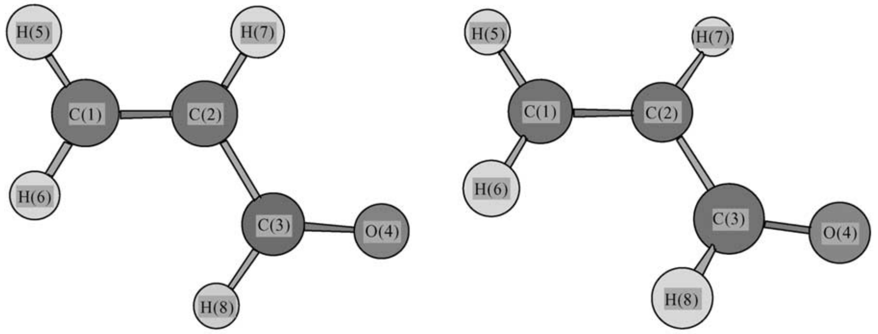

$C_3H_4O$
$C_{(1)}$-$C_{(2)}$=1.338 $C_{(2)}$-$C_{(3)}$=1.475 $C_{(3)}$-$O_{(4)}$=1.215
$\angle C_{(1)}C_{(2)}C_{(3)}O_{(4)}$=180.0

$C_3H_4O^{+\bullet}$ ($1^+$, trans-)
$C_{(1)}$-$C_{(2)}$=1.354 $C_{(2)}$-$C_{(3)}$=1.439 $C_{(3)}$-$O_{(4)}$=1.234
$\angle C_{(1)}C_{(2)}C_{(3)}O_{(4)}$=180.0

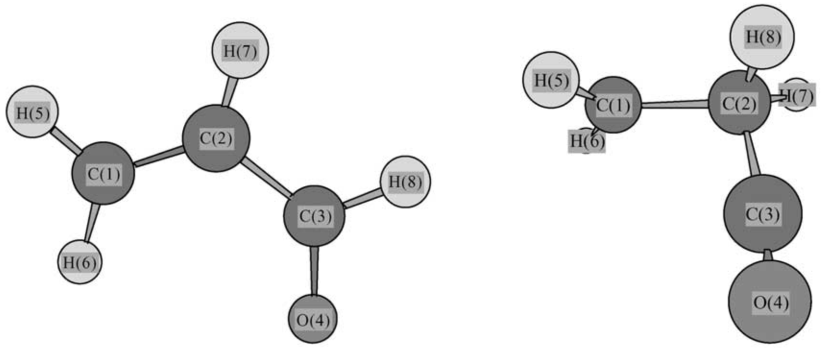

$C_3H_4O^{+\bullet}$ ($1^+$, cis-)
$C_{(1)}$-$C_{(2)}$=1.355 $C_{(2)}$-$C_{(3)}$=1.445 $C_{(3)}$-$O_{(4)}$=1.232
$\angle C_{(1)}C_{(2)}C_{(3)}O_{(4)}$=0.0

$C_3H_4O^{+\bullet}$ ($2^+$)
$C_{(1)}$-$C_{(2)}$=1.507 $C_{(2)}$-$C_{(3)}$=1.459 $C_{(3)}$-$O_{(4)}$=1.129
$\angle C_{(1)}C_{(2)}C_{(3)}O_{(4)}$=0.7

Fig. 1. Equilibrium structures and main parameters obtained at the B3LYP/6-31G* level ($TS_{13}$(a) and $TS_{47}$ were obtained at the HF/6-31G* level).

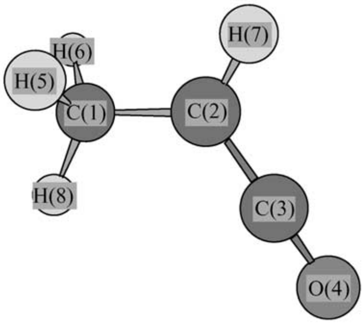

$C_3H_4O^{+\bullet}$ ($3^+$)
$C_{(1)}$-$C_{(2)}$=1.483 $C_{(2)}$-$C_{(3)}$=1.382 $C_{(3}$-$O_{(4)}$=1.139
$\angle C_{(1)}C_{(2)}C_{(3)}O_{(4)}$=0.0

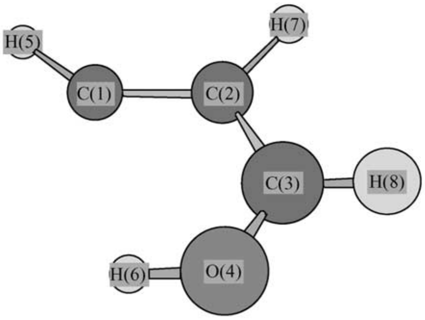

$C_3H_4O^{+\bullet}$ ($4^+$)
$C_{(1)}$-$C_{(2)}$=1.335 $C_{(2)}$-$C_{(3)}$=1.430 $C_{(3}$-$O_{(4)}$=1.279
$\angle C_{(1)}C_{(2)}C_{(3)}O_{(4)}$=0.0

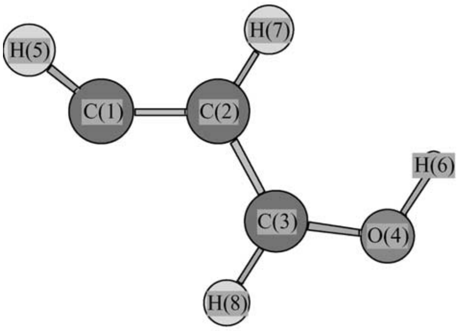

$C_3H_4O^{+\bullet}$ ($5^+$)
$C_{(1)}$-$C_{(2)}$=1.339 $C_{(2)}$-$C_{(3)}$=1.420 $C_{(3}$-$O_{(4)}$=1.281
$\angle C_{(1)}C_{(2)}C_{(3)}O_{(4)}$=180.0

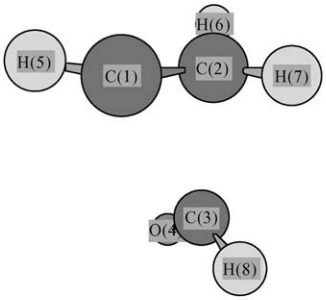

$C_3H_4O^{+\bullet}$ ($6^+$)
$C_{(1)}$-$C_{(2)}$=1.350 $C_{(2)}$-$C_{(3)}$=1.960 $C_{(3}$-$O_{(4)}$=1.154
$\angle C_{(1)}C_{(2)}C_{(3)}$=92.6 $\angle C_{(1)}C_{(2)}C_{(3)}O_{(4)}$=99.6

Fig. 1. (*Continued*).

with the B3LYP/6-31G* method. On the other hand, the HF/6-31G* calculation generated relative energies that differed considerably. The relative energies of the isomers, transition states and dissociation products obtained at the B3LYP/6-311+G**//B3LYP/6-31G* level are shown in Fig. 2.

The C=C–C=O backbone of the acrolein molecule can rotate about the single bond generating the *cis*- and *trans*-isomers in both the neutral and ionic forms. In neutral acrolein, the energy difference and barrier height between the lower energy *trans*- and the *cis*-isomers have been determined to be about 7 and 32 kJ/mol, respectively, by experimental (IR [28], Raman [29], UV spectroscopy [30,31], and microwave spectroscopy [32]) and theoretical methods (ab initio [33,34] and DFT calculations [35]), which are in good agreement with each other. There are no experimental data for rotation of the acrolein ion. However, unrestricted HF calculations [10] predicted that the *trans*-ion is more stable than the *cis*-structure by 8.4 kJ/mol. Our DFT calculations yield essentially the same energy difference, 9.1 kJ/mol. The transition state connecting the *cis*- and *trans*-acrolein ion structures, $TS_{tc}$, shows that the dihedral angle, $C_{(1)}$–$C_{(2)}$–$C_{(3)}$–O, varies from 0° in the *cis*-configuration to −110.8° in $TS_{tc}$, to

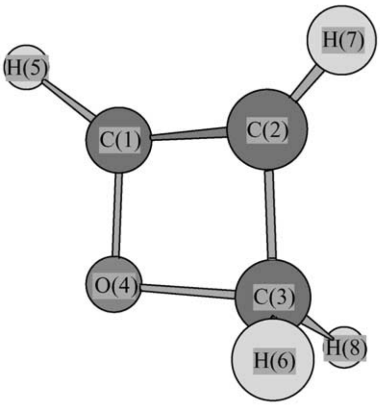

$C_3H_4O^{+\bullet}$ ($7^+$)
$C_{(1)}$-$C_{(2)}$=1.413 $C_{(2)}$-$C_{(3)}$=1.508 $C_{(3}$-$O_{(4)}$=1.531
$C_{(1)}$-$O_{(4)}$=1.305 $\angle C_{(1)}C_{(2)}C_{(3)}$=87.2 $\angle C_{(2)}C_{(3)}O_{(4)}$=84.8
$\angle C_{(1)}O_{(4)}C_{(3)}$=90.2 $\angle C_{(1)}C_{(2)}C_{(3)}O_{(4)}$=0.0

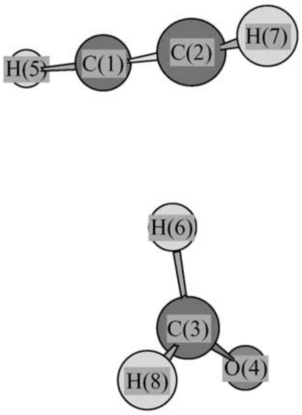

$C_3H_4O^{+\bullet}$ ($8^+$)
$C_{(1)}$-$C_{(2)}$=1.222 $H_{(6)}$-$C_{(1)}$=2.061 $H_{(6)}$-$C_{(2)}$=2.062
$H_{(6)}$-$C_{(3)}$=1.172 $\angle C_{(1)}C_{(2)}C_{(3)}O_{(4)}$=96.0

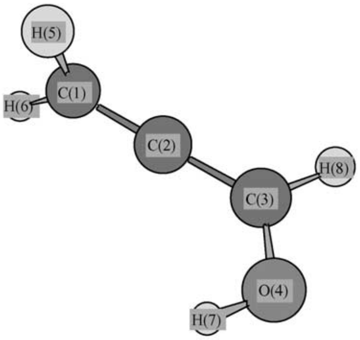

$C_3H_4O^{+\bullet}$ ($9^+$)
$C_{(1)}$-$C_{(2)}$=1.290 $C_{(2)}$-$C_{(3)}$=1.377 $C_{(3}$-$O_{(4)}$=1.302
$\angle C_{(1)}C_{(2)}C_{(3)}O_{(4)}$=180.0

Fig. 1. (*Continued*).

180° in the *trans*-form. The transition state energy of 26 kJ/mol relative to the *trans*-isomer is also very similar to its value in neutral acrolein. Since the *trans*-isomer is more stable than the *cis*- for both neutral and ionic acrolein, all relative energies are based on the *trans*-isomer.

As shown in Fig. 1, the distonic ion, $^{\bullet}CH_2CH_2CO^+$ (**2**$^+$) can be generated from acrolein by a hydrogen atom transfer from $C_{(3)}$ to $C_{(2)}$ via $TS_{12}$. The lowest energy structure of methylketene (**3**$^+$) can be obtained from acrolein by the transfer of a hydrogen atom from $C_{(3)}$ to $C_{(1)}$. However, as will be apparent, this is more efficiently achieved via two lower energy hydrogen atom transfer steps. The other two relatively low energy isomers are **4**$^+$ and **5**$^+$, which correspond to structures in which one of the hydrogen atoms on $C_{(1)}$ of the *cis*- and *trans*-acrolein are shifted to the oxygen atom, respectively. The conversion between **4**$^+$ and **5**$^+$ corresponds to an intermolecular rotation around the $C_{(2)}$–$C_{(3)}$ axis. Although this involves rotation

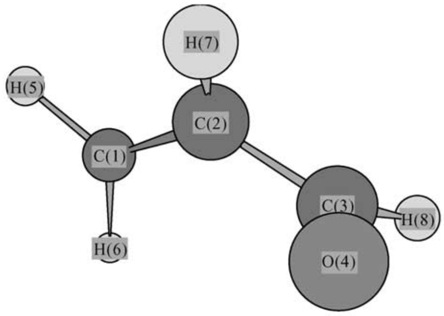

$TS_{tc}$
$C_{(1)}$-$C_{(2)}$=1.360 $C_{(2)}$-$C_{(3)}$=1.510 $C_{(3}$-$O_{(4)}$=1.210
$\angle C_{(1)}C_{(2)}C_{(3)}O_{(4)}$=-110.8

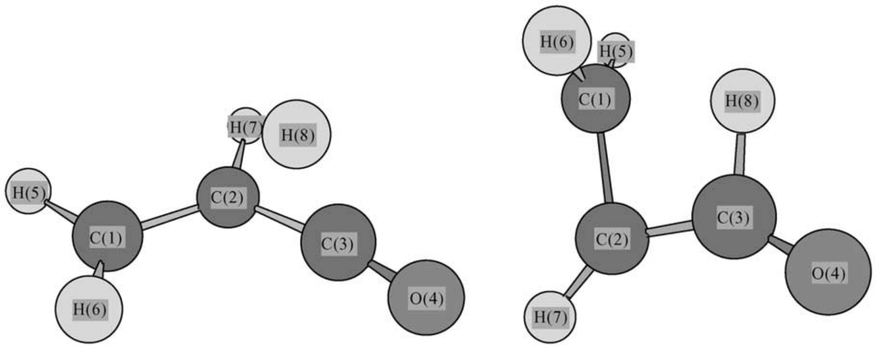

$TS_{12}$
$C_{(1)}$-$C_{(2)}$=1.407 $C_{(2)}$-$C_{(3)}$=1.407 $H_{(8)}$-$C_{(2)}$=1.524 $H_{(8)}$-$C_{(3)}$=1.361 $\angle H_{(8)}C_{(2)}C_{(3)}$=55.2 $\angle H_{(8)}C_{(3)}C_{(2)}$=66.8
$\angle C_{(1)}C_{(2)}C_{(3)}O_{(4)}$=85.4

$TS_{13}$ (a)
$C_{(1)}$-$C_{(2)}$=1.483 $C_{(2)}$-$C_{(3)}$=1.381 $C_{(3}$-$O_{(4)}$=2.444 $H_{(8)}$-$C_{(1)}$=1.632 $H_{(8)}$-$C_{(3)}$=1.215 $\angle C_{(1)}C_{(2)}C_{(3)}H_{(8)}$=0.0
$\angle C_{(1)}C_{(2)}C_{(3)}O_{(4)}$=-179.3

Fig. 1. (*Continued*).

around the same bond as in the *cis–trans* conversion in acrolein, the barrier for $TS_{45}$ is calculated to be considerably higher (60 kJ/mol rather than 26 kJ/mol), a change that is not reflected in the $C_{(2)}$–$C_{(3)}$ bond lengths, which remain about the same for $\mathbf{1}^+$ and $\mathbf{4}^+$. The $\mathbf{6}^+$ ion is an ion–dipole complex of $C_2H_3{}^+$ and $HCO^\bullet$ or $C_2H_3{}^\bullet$ and $HCO^+$. As shown in Fig. 2(b), its energy of 159.1 kJ/mol lies about 1 eV below its dissociation products. The Mulliken population analysis shows that the total atomic charges on $C_2H_3$ and HCO are very similar, 0.53 and 0.47, respectively, which suggests that this ion dissociates to both of the products.

Isomer $\mathbf{7}^+$ is a four-membered ring whose energy lies just 30.2 kJ/mol above the acrolein ion. Isomer $\mathbf{8}^+$ is another ion–dipole complex, this time between $C_2H_2$ and $H_2CO^{\bullet+}$. The distance between $H_{(6)}$ and the two carbon atoms in the acetylene molecule is 2.06 Å, far larger than a normal C–H bond of 1 Å, while the $H_{(6)}$–$C_{(3)}$ bond in the formaldehyde ion is 1.17 Å. Its energy lies some 102 kJ/mol below its dissociation products. Isomer $\mathbf{9}^+$ (the hydroxyallene ion)

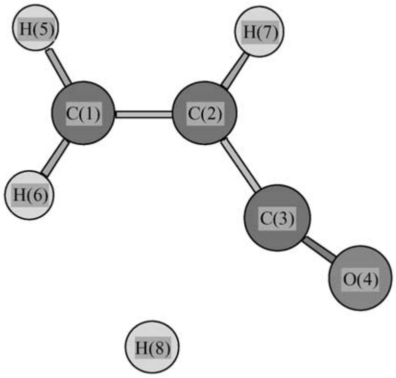

$TS_{13}$ (b)
$C_{(1)}$-$C_{(2)}$=1.349 $C_{(2)}$-$C_{(3)}$=1.413 $C_{(3}$-$O_{(4)}$=1.141 $H_{(6)}$-
$H_{(8)}$=2.177 $H_{(8)}$-$C_{(3)}$=1.988 $\angle C_{(1)}C_{(2)}C_{(3)}H_{(8)}$=0.0
$\angle C_{(1)}C_{(2)}C_{(3)}O_{(4)}$=179.7

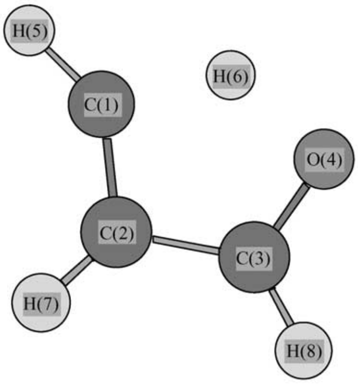

$TS_{14}$
$C_{(1)}$-$C_{(2)}$=1.341 $C_{(2)}$-$C_{(3)}$=1.448 $C_{(3)}$-$O_{(4)}$=1.266
$H_{(6)}$-$C_{(1)}$=1.373 $H_{(6)}$-$O_{(4)}$=1.302
$\angle H_{(6)}C_{(1)}C_{(2)}C_{(3)}$=0.0 $\angle C_{(1)}C_{(2)}C_{(3)}O_{(4)}$=0.0

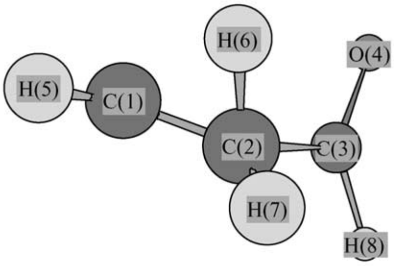

$TS_{16}$
$C_{(1)}$-$C_{(2)}$=1.352 $C_{(2)}$-$C_{(3)}$=1.602 $C_{(3)}$-$O_{(4)}$=1.187
$H_{(6)}$-$C_{(1)}$=1.481 $H_{(6)}$-$C_{(2)}$=1.214 $\angle H_{(6)}C_{(1)}C_{(2)}$=70.3
$\angle C_{(1)}C_{(2)}C_{(3)}O_{(4)}$=61.6

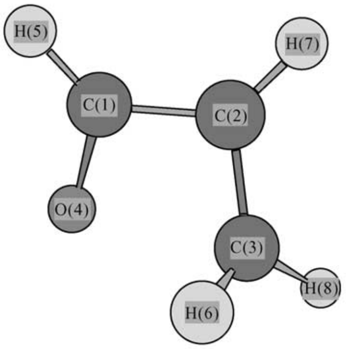

$TS_{17}$
$C_{(1)}$-$C_{(2)}$=1.421 $C_{(2)}$-$C_{(3)}$=1.441 $C_{(3)}$-$O_{(4)}$=2.016 $C_{(1)}$-
$O_{(4)}$=1.271 $H_{(6)}$-$C_{(3)}$=1.088 $H_{(6)}$-$O_{(4)}$=2.211
$\angle H_{(6)}C_{(3)}O_{(4)}$=85.3 $\angle H_{(6)}C_{(3)}C_{(2)}C_{(1)}$=-62.7
$\angle C_{(1)}C_{(2)}C_{(3)}O_{(4)}$=11.2

Fig. 1. (*Continued*).

corresponds to the structure in which the hydrogen atom on the $C_{(2)}$ carbon atom of the acrolein ion shifts to the oxygen atom. This ion is 12.8 kJ/mol more stable than the acrolein ion.

There are a number of other possible $C_3H_4O^{\bullet +}$ isomers that have been reported in the literature, which were not considered in this study. One suggested by Bouchoux [11] is an ion–dipole complex between $CH_2CH_2^{\bullet +}$ and CO, in which the oxygen atom points toward the ethylene ion. Although this isomer is stable, having an energy just 7.6 kJ/mol higher than $\mathbf{2}^+$ [11], its backbone structure of C–C–O–C rather than C–C–C–O means that it can probably be produced only via a high-energy barrier. Another isomer is $CH_2CHCOH^{\bullet +}$ (H on O rather than on $C_{(3)}$) [11]. Although its energy is almost equal to that of the acrolein ion, it does not dissociate directly to any of the probable products. The cyclopropanone ion that

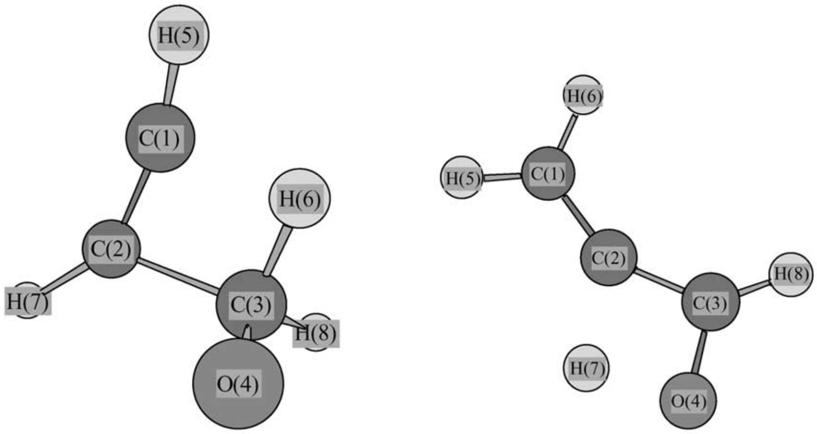

TS$_{18}$
$C_{(1)}$-$C_{(2)}$=1.272 $C_{(2)}$-$C_{(3)}$=1.572 $C_{(3}$-$O_{(4)}$=1.310 $H_{(6)}$-$C_{(1)}$=1.569 $H_{(6)}$-$C_{(3)}$=1.214 $\angle C_{(1)}C_{(2)}C_{(3)}H_{(6)}$=-1.9 $\angle C_{(1)}C_{(2)}C_{(3)}O_{(4)}$=111.9

TS$_{19}$
$C_{(1)}$-$C_{(2)}$=1.326 $C_{(2)}$-$C_{(3)}$=1.404 $C_{(3)}$-$O_{(4)}$=1.281 $H_{(7)}$-$C_{(2)}$=1.431 $H_{(7)}$-$O_{(4)}$=1.353 $\angle H_{(7)}C_{(2)}C_{(3)}O_{(4)}$=0.0 $\angle C_{(1)}C_{(2)}C_{(3)}O_{(4)}$=-180.0

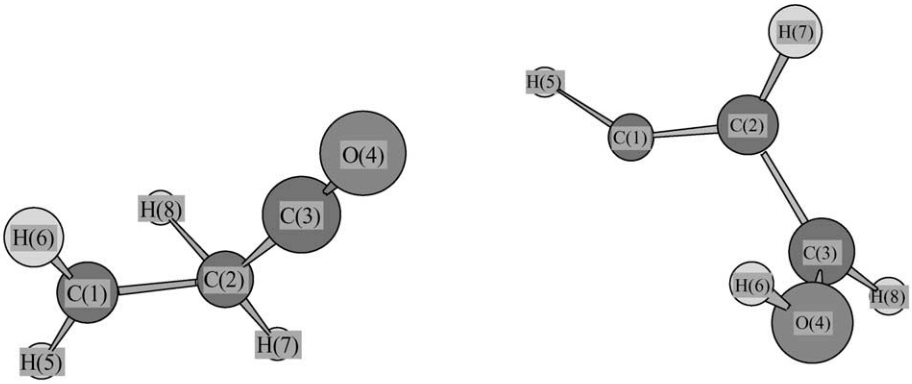

TS$_{23}$
$C_{(1)}$-$C_{(2)}$=1.472 $C_{(2)}$-$C_{(3)}$=1.392 $C_{(3)}$-$O_{(4)}$=1.143 $H_{(8)}$-$C_{(1)}$=1.442 $H_{(8)}$-$C_{(2)}$=1.228 $\angle H_{(8)}C_{(2)}C_{(1)}$=63.8 $\angle C_{(1)}C_{(2)}C_{(3)}O_{(4)}$=-100.5

TS$_{45}$
$C_{(1)}$-$C_{(2)}$=1.312 $C_{(2)}$-$C_{(3)}$=1.472 $C_{(3)}$-$O_{(4)}$=1.266 $\angle C_{(1)}C_{(2)}C_{(3)}O_{(4)}$=-92.3

Fig. 1. (*Continued*).

was considered by several workers [8,11,14], is probably according to MP2 level calculations, a transition state connecting two degenerate rearrangements of the distonic ion (**2**$^+$) [8]. An isomer found by McKee and Radom [8] is $^\bullet CH_2CH_2CO^+$ in the form of a four-membered ring with an energy at the G2 level of 155.7 kJ/mol above **2**$^+$.

The relative energies of the transition states connecting the various isomers are listed in Table 1 and shown graphically in Fig. 2. Some of them deserve special mention, among them TS$_{14}$. It is apparent that the transfer of $H_{(6)}$ from acrolein (**1**$^+$) to the **4**$^+$/**5**$^+$ structures can only occur from the *cis*- form of **1**$^+$. The transition state obtained is TS$_{14}$, which is a five-membered

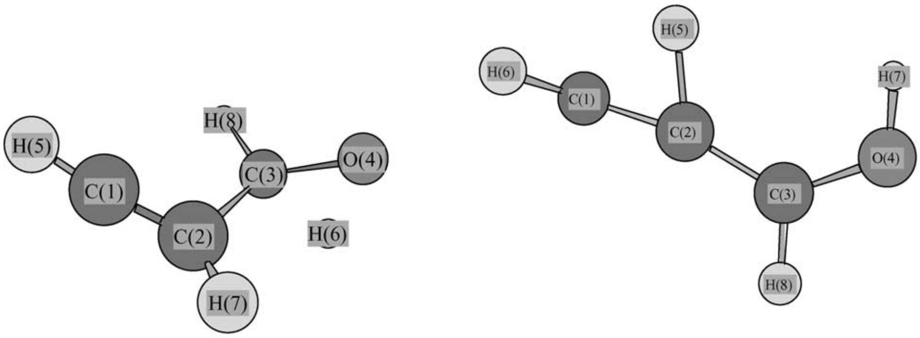

$TS_{58}$
$C_{(1)}$-$C_{(2)}$=1.280 $C_{(2)}$-$C_{(3)}$=1.536 $C_{(3)}$-$O_{(4)}$=1.312 $H_{(6)}$-$C_{(3)}$=1.248 $H_{(6)}$-$O_{(4)}$=1.352 $\angle H_{(6)}C_{(3)}O_{(4)}$=63.4 $\angle H_{(6)}O_{(4)}C_{(3)}$=55.8 $\angle C_{(1)}C_{(2)}C_{(3)}O_{(4)}$=135.7

$TS_{59}$
$C_{(1)}$-$C_{(2)}$=1.284 $C_{(2)}$-$C_{(3)}$=1.381 $C_{(3)}$-$O_{(4)}$=1.315 $H_{(5)}$-$C_{(1)}$=1.413 $H_{(5)}$-$C_{(2)}$=1.222 $\angle H_{(5)}C_{(2)}C_{(1)}$=68.6 $\angle C_{(1)}C_{(2)}C_{(3)}O_{(4)}$=151.8

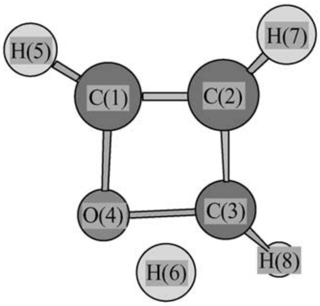

$TS_{47}$
$C_{(1)}$-$C_{(2)}$=1.359 $C_{(2)}$-$C_{(3)}$=1.441 $C_{(3)}$-$O_{(4)}$=1.446 $C_{(1)}$-$O_{(4)}$=1.483 $H_{(6)}$-$C_{(3)}$=1.260 $H_{(6)}$-$O_{(4)}$=1.333 $\angle H_{(6)}C_{(3)}O_{(4)}$=58.6 $\angle H_{(6)}C_{(3)}C_{(2)}C_{(1)}$=-57.5 $\angle C_{(1)}C_{(2)}C_{(3)}O_{(4)}$=0.0

Fig. 1. (*Continued*).

ring structure, in which $H_{(6)}$ is almost equidistant between $C_{(1)}$ and the oxygen atom. When $H_{(6)}$ is fully transferred, it generates the *cis*-isomer $\mathbf{4}^+$. Thus, to go from the *trans*- form of $\mathbf{1}^+$ to $\mathbf{5}^+$ requires first an isomerization to the *cis*- form of acrolein, the formation of $\mathbf{4}^+$ (*cis*-), followed by another isomerization to $\mathbf{5}^+$ (*trans*-).

We were not successful in finding the transition state, $TS_{13}$, which connects the acrolein ion directly with the methylketene ion at the DFT level. All attempts to move $H_{(8)}$ from the $C_{(3)}$ to the terminal carbon atom, resulted in the hydrogen atom leaving and forming the $C_3H_3O^+$ product. The structure $TS_{13}$(a) shown in Fig. 1 is the result obtained at the HF/6-31G* level, in which $H_{(8)}$ and the three carbon atoms form a distorted square. Further optimization at the B3LYP/6-31G* level yielded $TS_{13}$(b), in which $H_{(8)}$, the three carbon atoms, and $H_{(6)}$ form a nearly planar five-membered ring. Furthermore, the frequency analysis and IRC calculation show that this structure is more akin to a transition state for the hydrogen atom loss reaction, rather than $TS_{13}$. The DFT single point using the HF/6-31G* geometry gives the $TS_{13}$ relative energy of 201 kJ/mol, which is 118 kJ/mol higher than $TS_{12}$. Thus, as shown in Fig. 2(a), we assume that the methylketene ion is formed by two steps, the first one

Table 1
Energies, ZPE (in Hartree), $\langle S^2 \rangle$ and relative energies (in kJ/mol)

| Species | HF/6-31G* | | | | B3LYP/6-31G* | | | | B3LYP/6-311+G**(SP) | | Relative energy |
|---|---|---|---|---|---|---|---|---|---|---|---|
| | Energy | $\langle S^2 \rangle$ | ZPE | RE[a] | Energy | $\langle S^2 \rangle$ | ZPE | RE[a] | Energy | $\langle S^2 \rangle$ | |
| $C_3H_4O$(*trans*-) | −190.7624237 | – | 0.066458 | −805.1 | −191.9119736 | – | 0.061651 | −930.3 | −191.9741254 | – | −955.9 |
| $C_3H_4O^{\bullet+}(\mathbf{1}^+)$ | −190.4546195 | 0.844 | 0.065273 | 0 | −191.5557857 | 0.759 | 0.059946 | 0 | −191.6079922 | 0.759 | 0 |
| $C_3H_4O^{\bullet+}$(*cis*-) | −190.4507041 | 0.875 | 0.065005 | 9.6 | −191.5523482 | 0.759 | 0.059698 | 8.4 | −191.6042652 | 0.759 | 9.1 |
| $C_3H_4O^{\bullet+}(\mathbf{2}^+)$ | −190.4674588 | 0.762 | 0.063235 | −38.5 | −191.5711423 | 0.754 | 0.059371 | −41.8 | −191.6255818 | 0.754 | −47.7 |
| $C_3H_4O^{\bullet+}(\mathbf{3}^+)$ | −190.4798261 | 0.784 | 0.064415 | −68.2 | −191.5941682 | 0.755 | 0.060174 | −100.1 | −191.6485644 | 0.755 | −105.8 |
| $C_3H_4O^{\bullet+}(\mathbf{4}^+)$ | −190.4352687 | 1.021 | 0.065466 | 51.2 | −191.5366459 | 0.766 | 0.061099 | 53.5 | −191.5934959 | 0.765 | 41.1 |
| $C_3H_4O^{\bullet+}(\mathbf{5}^+)$ | −190.4387855 | 0.953 | 0.065625 | 42.4 | −191.5398437 | 0.764 | 0.061164 | 45.0 | −191.5970745 | 0.763 | 31.8 |
| $C_3H_4O^{\bullet+}(\mathbf{6}^+)$ | −190.3708464 | 1.014 | 0.060374 | 208.4 | −191.488645 | 0.766 | 0.056617 | 167.5 | −191.5439963 | 0.765 | 159.1 |
| $C_3H_4O^{\bullet+}(\mathbf{7}^+)$ | −190.4348669 | 0.784 | 0.067547 | 57.2 | −191.5504071 | 0.756 | 0.062755 | 21.5 | −191.5992802 | 0.756 | 30.2 |
| $C_3H_4O^{\bullet+}(\mathbf{8}^+)$ | −190.3581777 | 0.760 | 0.061283 | 243.8 | −191.4798375 | 0.756 | 0.052730 | 180.4 | −191.5399121 | 0.756 | 159.7 |
| $C_3H_4O^{\bullet+}(\mathbf{9}^+)$ | −190.4344159 | 0.992 | 0.065318 | 53.1 | −191.5549322 | 0.755 | 0.059953 | 2.3 | −191.6128705 | 0.755 | −12.8 |
| $TS_{tc}$ | −190.4296105 | 0.789 | 0.063673 | 61.9 | −191.5446567 | 0.762 | 0.059355 | 27.7 | −191.597398 | 0.762 | 26.2 |
| $TS_{12}$ | −190.3840143 | 0.820 | 0.058615 | 169.7 | −191.5137706 | 0.763 | 0.054803 | 96.7 | −191.5711898 | 0.763 | 83.0 |
| $TS_{13}$ | −190.3487707 | 0.951 | 0.058283 | 261.4 | – | – | – | – | −191.5235328 | 0.770 | 201.3[b] |
| $TS_{14}$ | −190.3658577 | 1.050 | 0.059124 | 218.5 | −191.4989304 | 0.761 | 0.055317 | 137.1 | −191.5539362 | 0.760 | 129.7 |
| $TS_{16}$ | – | – | – | – | −191.4691346 | 0.754 | 0.054105 | 212.1 | −191.5252688 | 0.755 | 201.7 |
| $TS_{17}$ | – | – | – | – | −191.5219699 | 0.769 | 0.060269 | 89.6 | −191.5718723 | 0.768 | 95.6 |
| $TS_{18}$ | −190.3149159 | 0.780 | 0.060592 | 355.7 | −191.4397271 | 0.756 | 0.054784 | 291.0 | −191.4962297 | 0.756 | 279.6 |
| $TS_{19}$ | −190.3380888 | 1.117 | 0.058301 | 289.5 | −191.4745638 | 0.764 | 0.054406 | 198.6 | −191.5298957 | 0.764 | 190.3 |
| $TS_{23}$ | −190.3979898 | 0.797 | 0.059800 | 135.8 | −191.53106 | 0.759 | 0.056321 | 55.4 | −191.5880561 | 0.758 | 42.8 |
| $TS_{45}$ | −190.4155664 | 0.974 | 0.063922 | 99.3 | −191.5133986 | 0.762 | 0.058912 | 108.5 | −191.5717007 | 0.761 | 92.5 |
| $TS_{47}$ | −190.2945504 | 1.049 | 0.058649 | 404.6 | – | – | – | – | −191.4855772 | 0.775 | 301.7[b] |
| $TS_{58}$ | −190.2959101 | 1.537 | 0.056993 | 397.1 | −191.4119194 | 0.794 | 0.052477 | 358.0 | −191.4691711 | 0.791 | 344.5 |
| $TS_{59}$ | −190.3610406 | 0.878 | 0.058101 | 228.8 | −191.4843819 | 0.764 | 0.054997 | 174.4 | −191.546305 | 0.764 | 148.8 |
| $C_3H_3O^+$ | −189.910042 | – | 0.054668 | – | −191.0091175 | – | 0.050877 | – | −191.0630134 | – | – |

[a] RE: relative energy with the ZPE corrections (scaled by 0.893 [27] at the HF/6-31G*).

[b] B3LYP/6-311+G**//HF/6-31G* results.

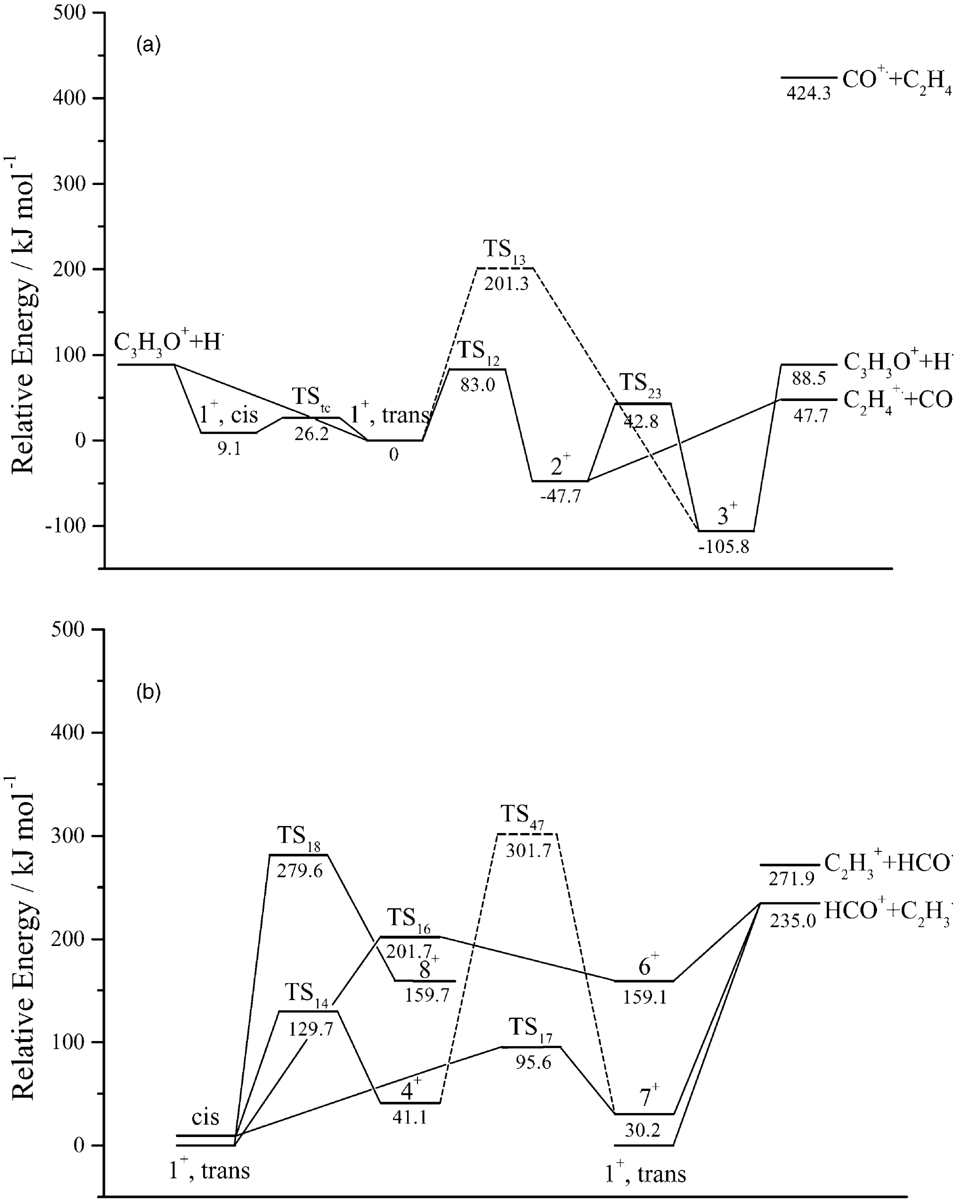

Fig. 2. Relative energy schematic diagram of the isomerization and dissociation reactions of the $C_3H_4O^{\bullet+}$ isomers (dashed line: the B3LYP/6-311+G**//HF/6-31G* results): (a) Dissociation channels, $C_2H_4^{\bullet+} + CO$, $C_3H_3O^+ + H^\bullet$, and $CO^{\bullet+} + C_2H_4$; (b) Dissociation channels, $HCO^+ + C_2H_3^\bullet$ and $C_2H_3^+ + HCO^\bullet$; (c) Dissociation channels, $H_2CO^{\bullet+} + C_2H_2$ and $C_2H_2^{\bullet+} + H_2CO$; (d) Dissociation channels, $HCOH^{\bullet+} + C_2H_2$ and $C_2H_2^{\bullet+} + HCOH$.

producing the distonic (**2**$^+$) ion followed by a second hydrogen atom transfer step to **3**$^+$. A similar situation arose in our search for $TS_{47}$. Optimization at the HF level produced a four-membered ring structure, which seemed poised to decay to the four-membered ring, **7**$^+$. However, further optimization with DFT (B3LYP/6-31G*) converted this structure into a transition state connecting **1**$^+$ and **7**$^+$, $TS_{17}$.

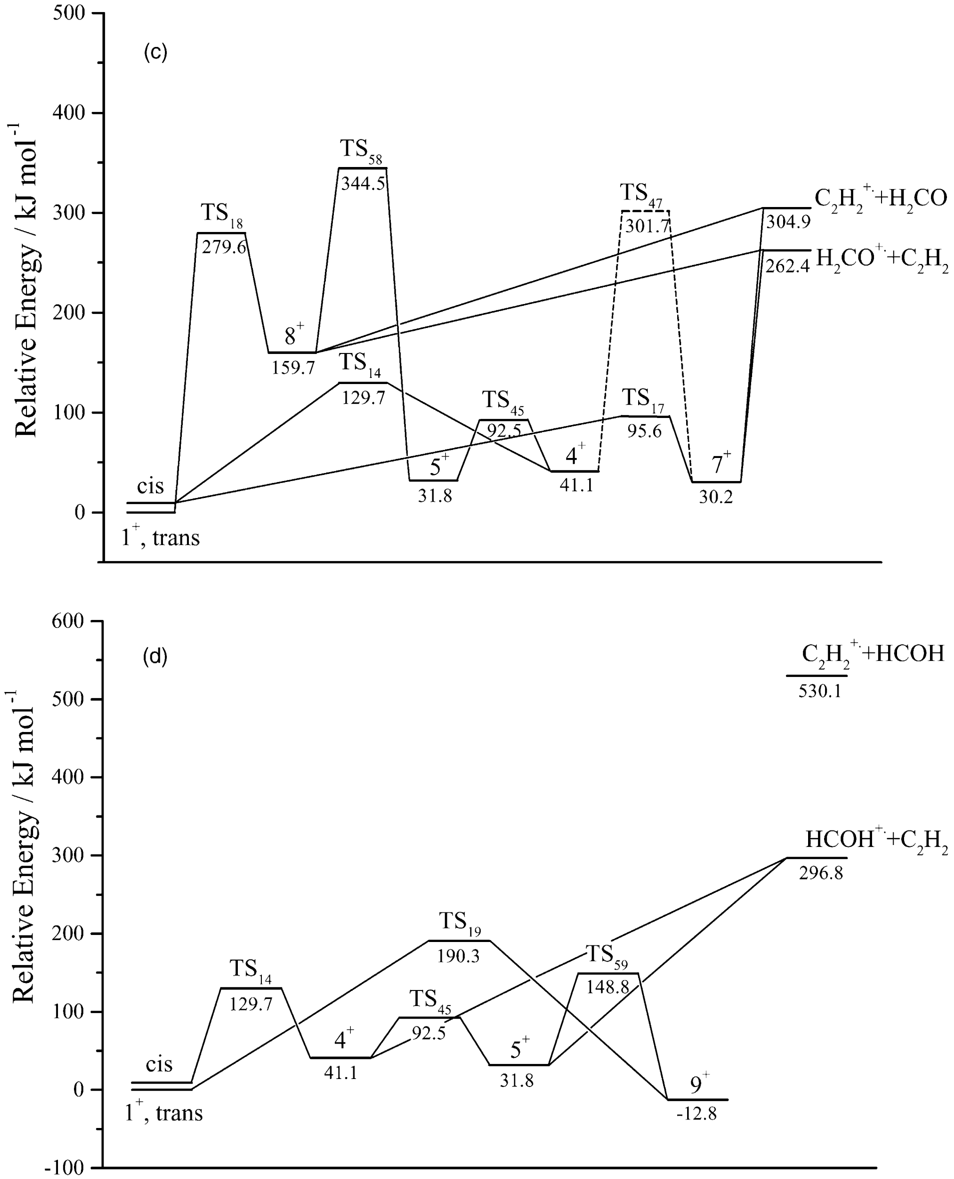

Fig. 2. (*Continued*).

### *3.2. Dissociation channels and dissociation energies*

Fig. 2 show the nine dissociation channels along with the transition states that connect the various isomeric structures to the products.

#### *3.2.1.* $C_2H_4^{\bullet +} + CO$ *(or* $CO^{\bullet +} + C_2H_4$*) and* $C_3H_3O^+ + H^\bullet$

The thermochemically lowest energy dissociation channels of the acrolein ion are via CO and H$^\bullet$ loss. Because the transition states leading to these products have low energies, these channels are experimentally observed as the lowest energy ion products [12,14,36]. The $H^{\bullet}$ loss product has the structure $CH_2CHCO^+$ [37], which can be reached by a simple hydrogen atom loss from the terminal $C_{(3)}$ carbon atom of the acrolein ion. On the other hand, the CO loss channel requires a prior isomerization to the distonic ion, $^{\bullet}CH_2CH_2CO^+$ (**2**$^+$) that is reached by a hydrogen atom transfer from $C_{(3)}$ to $C_{(2)}$. This structure can be produced via the transition state, $TS_{12}$, whose energy is 83 kJ/mol above the acrolein ion energy. According to our calculations, ion **2**$^+$ lies $-47.7$ kJ/mol below the acrolein ion. This result is close to the value reported by Bouchoux ($-34$ kJ/mol) [11], but 25 kJ/mol higher than $-72.8$ kJ/mol calculated by McKee and Radom [8]. The methylketene ion, $CH_3CHCO^{\bullet+}$ (**3**$^+$) is also expected to play a role in this reaction. Although it does not lead directly to the $C_2H_4^{\bullet+}$ product, the transition state, $TS_{23}$, that converts **2**$^+$ into **3**$^+$, lies below the CO loss product channel so that the methylketene ion may be formed during the course of the CO loss reaction. In addition, the $H^{\bullet}$ loss product can be formed directly from methylketene simply by the loss of a hydrogen atom from the terminal carbon atom, $C_{(1)}$. The methylketene ion has the lowest energy of all the $C_3H_4O^{\bullet+}$ structures. Our calculations suggest an energy of $-105.8$ kJ/mol relative to the acrolein ion, which is close to the G2 value of $-120.8$ kJ/mol reported by McKee and Radom [8]. The Bouchoux value using a single point 6-31G(d,p) calculation at a geometry calculated with the 3-21G basis set was $-64$ kJ/mol [11].

As shown in Fig. 2(a), the $H^{\bullet}$ loss product can be produced without an energy limiting barrier, while the CO loss product is predicted to be formed at an energy of 35 kJ/mol ($TS_{12}$) above its dissociation limit. However, because the transition state involves the transfer of a hydrogen atom, it is very likely that tunneling will lower the effective barrier by several kJ/mol.

### 3.2.2. $HCO^+ + C_2H_3^{\bullet}$ and $C_2H_3^+ + HCO^{\bullet}$

The lowest energy structures for $C_2H_3^{\bullet}$ and $C_2H_3^+$ are quite different in that the ion, as determined by coulomb explosion studies, has a hydrogen bridged structure [38]. However, its calculated energy at the MP2/6-31G* level of theory is just 13 kJ/mol below that of the classical non-bridged ion structure [39]. Our DFT calculation suggested a smaller energy difference of 1.5 kJ/mol and a barrier of 2.3 kJ/mol.

The production of $HCO^{\bullet}$ (or $HCO^+$) and $C_2H_3^+$ (or $C_2H_3^{\bullet}$) from the acrolein ion does not, in principle, involve any rearrangement because it could react by a simple $C_{(2)}$–$C_{(3)}$ bond rupture. A possible precursor for the production of these products is ion **7**$^+$, whose structure is a four-membered ring with an energy that is only 30.2 kJ/mol higher than the acrolein ion energy. Moreover, the production of isomer **7**$^+$ is easily accomplished from the acrolein ion through the low energy transition state, $TS_{17}$.

The other two possible precursors are ions **6**$^+$ and **8**$^+$. As shown in Fig. 2(b) the reaction can proceed via $TS_{16}$ to generate an ion–dipole complex (**6**$^+$) between $HCO^+$ and $C_2H_3^{\bullet}$, or $HCO^{\bullet}$ and $C_2H_3^+$. The charge on this isomer **6**$^+$ is located almost equally on the HCO and the $C_2H_3$ units. Oddly enough, the $TS_{16}$ shows that $H_{(6)}$ has migrated from the terminal carbon to $C_{(2)}$, which indicates that this reaction proceeds not by a simple C–C bond break, but by a prior hydrogen atom transfer reaction. Unfortunately, the product $C_2H_3^+$ contains no clues concerning the validity of this mechanism since the structure is identical with or without the hydrogen atom transfer. For ion **8**$^+$, the production of the $[C_2H_3 + HCO]^{\bullet+}$ products corresponds to a cleavage process of the $C_{(3)}$–$H_{(6)}$ bond.

### 3.2.3. $H_2CO^{\bullet+} + C_2H_2$ and $C_2H_2^{\bullet+} + H_2CO$

The two product channels involving ions of formaldehyde and acetylene can originate via simple bond ruptures from isomers **7**$^+$ or **8**$^+$. The latter is an ion–neutral complex between $C_2H_2$ and $H_2CO^{\bullet+}$. Structure **8**$^+$ is formed by a 1,3-H migration process via a transition state, $TS_{18}$, lying at 279.6 kJ/mol relative to the acrolein ion. This energy barrier is only a little higher than the lower dissociation channel energy. As discussed above, isomer **7**$^+$, 130 kJ/mol more stable than **8**$^+$, can be directly produced from *cis*-**1**$^+$ through a low energy barrier.

#### 3.2.4. $HCOH^{\bullet +}$ (hydroxymethylene ion) + $C_2H_2$ and $C_2H_2^{\bullet +}$ + HCOH

Although the production of $C_2H_2^{\bullet +}$ + HCOH is a very high energy process, the charge transfer product, $HCOH^{\bullet +}$ + $C_2H_2$ reaction is close in energy to the formaldehyde and acetylene product channels (Fig. 2(c)). In addition, the formation of good precursors for this channel involves lower energy barriers (Fig. 2(d)). Both $\mathbf{4}^+$ and $\mathbf{5}^+$ are candidates for the immediate precursor to the hydroxymethylene ion and acetylene channels. Fig. 2(d) shows that the lowest energy reaction pathway is $\mathbf{1}^+$ (*cis*-) → $\mathbf{4}^+$ → dissociation products.

### 3.3. The thermochemical results

Table 2 lists the heats of formation of all the species obtained in this study. The calculated energies were converted to heats of formation by scaling them to the best known heats of formation, which are those of the products $C_2H_4^{\bullet +}$ and CO. The conversion between the 298 and 0 K heats of formation used the following equation:

$$\Delta_f H^\circ_{298\,K} - \Delta_f H^\circ_{0\,K} = [H^\circ_{298\,K} - H^\circ_{0\,K}] - [H^\circ_{298\,K} - H^\circ_{0\,K}]\,(\text{elements})$$

in which the $[H^\circ_{298\,K} - H^\circ_{0\,K}]$ values were calculated using vibrational frequencies obtained from the DFT calculation. The enthalpy changes of the elements in their standard states, $[H^\circ_{298\,K} - H^\circ_{0\,K}]$ (elements), were calculated using the following values: C(s): 1.050 kJ/mol, $H_2$(g): 8.468 kJ/mol, and $O_2$(g): 8.680 kJ/mol [43].

In the case of $C_3H_3O^+ + H^\bullet$, the heat of formation of the $CH_2CHCO^+$ ion was obtained by subtracting the known heat of formation of the hydrogen atom from the total. This yields a $\Delta_f H^\circ_{298\,K}[CH_2CHCO^+]$ of 779 kJ/mol, a value that is about 27 kJ/mol higher than the average of the older experimental values [12,37,40] that are listed in Table 2. In the accompanying TPEPICO study [36], we determined an upper limit to the heat of formation of the $CH_2CHCO^+$ ion of 783 kJ/mol, which is higher than the previous experimental results, but agrees with the present calculated energy. This is discussed more fully in the accompanying experimental paper.

Similarly, using the heats of formation of $HCO^\bullet$ ($HCO^+$) and $C_2H_2$ ($C_2H_2^{\bullet +}$); the heats of formation of $C_2H_3^\bullet$ ($C_2H_3^+$), $H_2CO$ ($H_2CO^{\bullet +}$), and HCOH ($HCOH^{\bullet +}$) were obtained. Because in each case, the heat of formation is scaled to the sum of the ion and neutral products, we arbitrarily distributed the error equally between the two species. This was done because all of the products have reasonably well established heats of formation. As shown in Table 2, the errors in the calculated values are +10 and +20 kJ/mol for the $HCO^+/C_2H_3^\bullet$ and $C_2H_3^+/HCO^\bullet$ products, respectively. In contrast the agreement between our calculations for the $[C_2H_2/H_2CO]^{\bullet +}$ system is within 4 kJ/mol, while the agreement with other calculated values for the $[C_2H_2/HCOH]^{\bullet +}$ system is also not too bad.

For the $C_3H_4O^{\bullet +}$ isomer, $\mathbf{1}^+$, the present theoretical result is similar to values of Bouchoux and Hoppilliard [48] and Lias et al. [40], and only 12 kJ/mol lower than the G2 result [8]. The neutral acrolein molecule energy was determined by subtracting the experimental IE of 10.11 eV from the ionic heat of formation. The value of −72 kJ/mol compares well with other theoretical values, namely the G2 calculation at −67.6 kJ/mol, and an MM3 value of −66 kJ/mol [49].

The calculated heat of formation of the distonic ion, $\mathbf{2}^+$, is 13.5 kJ/mol higher than the G2 result [8]. There are no good experimental energies for this ion, and our TPEPICO results also did not provide us with a value. On the other hand, methylketene and its ion ($\mathbf{3}^+$) have been extensively studied by experiments [9,20,51,53] and theoretical calculations [8,50,52,54]. Because no experimental heat of formation for the neutral is available, the heat of formation of the ion from the measured IE [20] depends on estimated energies of the neutral leading to a heat of formation of 759 kJ/mol [40]. Traeger [12,53] determined a somewhat higher energy of 778.7 kJ/mol, based on the appearance energy of $\mathbf{3}^+$ from several precursors, while Aubry et al. [51] reported a value of 765 kJ/mol. Recently, Traeger [9] redetermined the heat of formation

Table 2
Thermochemical results (in kJ/mol)[a]

| Species | $\Delta_f H^\circ_{298\,K}$ [b] | $\Delta_f H^\circ_{0\,K}$ [c] | $H^\circ_{298\,K} - H^\circ_{0\,K}$ [d] | Other results of $\Delta_f H^\circ_{298\,K}$ [e] |
|---|---|---|---|---|
| $C_2H_4^{\bullet+}$ | 1067.24 | 1075.365[f] | 10.91 | – |
| CO | −110.53 ± 0.17[g] | −113.82 ± 0.17[h] | 8.677 | – |
| $H^\bullet$ | 217.998 ± 0.006[g] | 216.035 ± 0.006[h] | 6.197[i] | – |
| $C_3H_3O^+$ | 779 | 786 | 13.33 | **751**[j], **749 ± 5**[k], **755.9**[l], **783 ± 10**[m] |
| $HCO^\bullet$ | 63 | 63 | 9.983[i] | **42**[n] |
| $HCO^+$ | 836 | 836 | 10.19 | **824**[g], **825.8**[o] |
| $C_2H_3^\bullet$ | 310 | 313 | 10.61 | **299.0 ± 5.0**[g,n], **265.3 ± 4**[j] |
| $C_2H_3^+$ | 1119 | 1123 | 11.47 | **1095 ± 13**[g] |
| $C_2H_2$ | 229 | 230 | 10.01[i] | **226.73**[i] |
| $C_2H_2^{\bullet+}$ | 1326 | 1326 | 10.90 | **1327.9**[j] |
| $H_2CO$ | −111 | −107 | 10.02[i] | **−108.6**[i] |
| $H_2CO^{\bullet+}$ | 943 | 947 | 10.19 | **941.8**[g] |
| HCOH | 114 | 118 | 10.06 | 113[p] |
| $HCOH^{\bullet+}$ | 977 | 981 | 10.19 | **962**[j], **968**[q] |
| $C_3H_4O^{\bullet+}$(**1**) | 904 | 914 | 14.06 | 916.3[r], 900[s] |
| $C_3H_4O$ (**1**) | −72 | −61 | 13.91 | −67.6[r], −66[t] |
| $C_3H_4O^{\bullet+}$(**2**) | 857 | 866 | 15.23 | 843.5[r] |
| $C_3H_4O^{\bullet+}$(**3**) | 799 | 808 | 15.18 | **759**[j], **778.7**[l], 797[r,u], **763**[s], 765 ± 5[v], 795[w], **783.5 ± 0.3**[x] |
| $C_3H_4O^{\bullet+}$(**4**) | 945 | 955 | 14.05 | – |
| $C_3H_4O^{\bullet+}$(**5**) | 936 | 946 | 14.09 | – |
| $C_3H_4O^{\bullet+}$(**6**) | 1065 | 1073 | 16.88 | – |
| $C_3H_4O^{\bullet+}$(**7**) | 932 | 944 | 12.09 | 920.1[r] |
| $C_3H_4O^{\bullet+}$(**8**) | 1069 | 1074 | 19.67 | – |
| $C_3H_4O^{\bullet+}$(**9**) | 892 | 901 | 15.25 | 906.0[r] |

[a] In the $H^\circ_{298\,K} - H^\circ_{0\,K}$ calculations, the heat capacity of electron was treated as 0.0 kJ/mol at all temperatures (the ion convention [40]). In order to convert to the electron convention, which treats the electron as a real particle, 6.197 kJ/mol should be added to the 298 K heat of formation each ion.

[b] $\Delta H^\circ_{0\,K} \rightarrow \Delta H^\circ_{298\,K}$.

[c] This study.

[d] Determined from the DFT calculated vibrational frequencies.

[e] The values in bold are the experimental results.

[f] $\Delta H^\circ_{0\,K(\mathrm{Ion})} = \Delta H^\circ_{0\,K(\mathrm{Neutral})} + \mathrm{IE}$, and the IE value is $10.5138 \pm 0.0006$ eV [41], and $\Delta H^\circ_{0\,K(\mathrm{Neutral})} = 60.938$ kJ/mol, which is derived by $\Delta H^\circ_{298\,K} \rightarrow \Delta H^\circ_{0\,K}$, and $\Delta_f H^\circ_{298\,K} = 52.467$ kJ/mol [42].

[g] NIST Webbook [41].

[h] $\Delta H^\circ_{298\,K} \rightarrow \Delta H^\circ_{0\,K}$.

[i] Wagman et al. [43].

[j] Lias et al. [40].

[k] Holmes et al. [37].

[l] Traeger et al. [12].

[m] Li and Baer [36].

[n] Tsang [44]

[o] Traeger and Kompe [45].

[p] Li and Schlegel [46].

[q] Ma et al. [47].

[r] McKee and Radom [8].

[s] Bouchoux and Hoppilliard [48].

[t] Allinger et al. [49].

[u] Scott and Radom [50].

[v] Aubry et al. [51].

[w] Nguyen et al. [52].

[x] Traeger [9].

of the ionic methylketene using threshold photoionization mass spectrometry. Using the appearance energies obtained from several difference precursors, he determined the heat of formation of the methylketene ion to be 783.5 kJ/mol, which is close to the most recent and high level theoretical results [50,52]. The G2 and our DFT calculations of the methylketene ion are in remarkably good agreement yielding 298 K heats of formation of 797 and 799 kJ/mol, respectively. The fact that several calculations at different levels of theory and experimental results all agree, seems good evidence a value of 790 ± 10 kJ/mol is the heat of formation of the methylketene ion.

Of the remaining $C_3H_4O^{\bullet+}$ structures listed in Table 2, ions **7**$^+$ and **9**$^+$ have also been calculated by G2 methods [8]. The DFT values differ from the G2 energies by about 13 kJ/mol, in one case lower and in the other higher.

## 4. Conclusions

The present calculations at the B3LYP/6-311+G**// B3LYP/6-31G* level provide the following results:

1. For the acrolein ion, the energy difference between the *trans–cis* isomers is 9.1 kJ/mol, and the energy barrier height is 26.2 kJ/mol, which is 6 kJ/mol lower than the neutral.
2. The structures **2**$^+$, **3**$^+$, and **9**$^+$ have lower energies than the acrolein ion, and **3**$^+$ is the most stable $C_3H_4O^{\bullet+}$ isomer.
3. Nine probable dissociation channels and dissociation energies were calculated. The fragments, $C_2H_4^{\bullet+}$ + CO, correspond to the lowest dissociation energy channel, which is preceded by a hydrogen migration from $C_{(3)}$ to $C_{(2)}$.
4. The product ions with the mass number, 30, may be the formaldehyde ion ($H_2CO^{\bullet+}$) or the hydroxymethylene ion ($HCOH^{\bullet+}$). The energy difference between the two channels is only about 34 kJ/mol.
5. The heats of formation of the $C_3H_4O^{\bullet+}$ isomers (**1**$^+$ → **9**$^+$) are calculated to be 904, 857, 799, 945, 936, 1065, 932, 1069 and 892 kJ/mol, respectively. By comparison with other available results, the average deviation of this study is estimated to be 10 kJ/mol and the maximum deviation is 30 kJ/mol.

## Acknowledgements

We thank the NC supercomputer facility for a generous allotment of computer time, and the U.S. Department of Energy, Office of Basic Energy Sciences, for support of this work.

## References

[1] K.W. Paulisse, T.O. Friday, M.L. Graske, W.F. Polik, J. Chem. Phys. 113 (2000) 184.
[2] Y. Hamada, Y. Nishimura, M. Tsuboi, Chem. Phys. 100 (1985) 365.
[3] P.K. Chowdhury, Chem. Phys. 260 (2000) 151.
[4] H. Shinohara, N. Nishi, J. Chem. Phys. 77 (1982) 234.
[5] B.M. Haas, T.K. Minton, P. Felder, J.R. Huber, J. Phys. Chem. 95 (1991) 5149.
[6] W.H. Fang, J. Am. Chem. Soc. 121 (1999) 8376.
[7] M. Reguero, M. Olivucci, F. Bernardi, M.A. Robb, J. Am. Chem. Soc. 116 (1994) 2103.
[8] M.L. McKee, L. Radom, Org. Mass Spectrom. 28 (1993) 1238.
[9] J.C. Traeger, Int. J. Mass Spectrom. 194 (2000) 261.
[10] T. Nakano, K. Morihashi, O. Kikichi, J. Mol. Struct. (Theochem.) 253 (1992) 161.
[11] G. Bouchoux, J. Mol. Struct. (Theochem.) 151 (1987) 107.
[12] J.C. Traeger, C.E. Hudson, D.J. McAdoo, Org. Mass Spectrom. 24 (1989) 230.
[13] F. Turecek, D.E. Drinkwater, F.W. McLafferty, J. Am. Chem. Soc. 113 (1991) 5958.
[14] F. Turecek, D.E. Drinkwater, F.W. McLafferty, J. Am. Chem. Soc. 113 (1991) 5950.
[15] H. Bock, S. Mohmand, T. Hirabayashi, A. Semkow, Chem. Ber. 115 (1982) 1339.
[16] A. Katrib, J.W. Rabalais, J. Phys. Chem. 77 (1973) 2358.
[17] P. Masclet, G. Mouvier, J. Electron Spectrosc. Relat. Phenom. 14 (1978) 77.
[18] H.V. Dam, A. Oskam, J. Electron Spectrosc. Relat. Phenom. 13 (1978) 273.
[19] W.V. Niessen, G. Bieri, L. Asbrink, J. Electron Spectrosc. Relat. Phenom. 21 (1980) 175.
[20] H. Bock, T. Hirabayashi, S. Mohmand, Chem. Ber. 114 (1981) 2595.
[21] R.I. Reed, M.B. Thornley, Trans. Faraday Soc. 54 (1958) 949.

[22] M.A. Haney, J.L. Franklin, J. Chem. Soc. Faraday Trans. 65 (1969) 1794.
[23] T.W. Shannon, A.G. Harrison, Can. J. Chem. 39 (1961) 1392.
[24] M.J. Frisch, G.W. Trucks, H.B. Schlegel, G.E. Scuseria, M.A. Robb, J.R. Cheeseman, V.G. Zakrzewski, J.A. Montgomery, R.E. Stratmann, J.C. Burant, S. Dapprich, J.M. Millam, A.D. Daniels, K.N. Kudin, M.C. Strain, Ö. Farkas, J. Tomasi, V. Barone, M. Cossi, R. Cammi, B. Mennucci, C. Pomelli, C. Adamo, S. Clifford, J. Ochterski, G.A. Petersson, P.Y. Ayala, Q. Cui, K. Morokuma, D.K. Malick, A.D. Rabuck, K. Raghavachari, J.B. Foresman, J. Cioslowski, J.V. Ortiz, A.G. Baboul, B.B. Stefanov, G. Liu, A. Liashenko, P. Piskorz, I. Komáromi, R. Gomperts, R.L. Martin, D.J. Fox, T. Keith, M.A. Al-Laham, C.Y. Peng, A. Nanayakkara, C. Gonzalez, M. Challacombe, P.M.W. Gill, B.G. Johnson, W. Chen, M.W. Wong, J.L. Andres, M. Head-Gordon, E.S. Replogle, J.A. Pople, GAUSSIAN 98, Revision A.7, Gaussian, Inc., Pittsburgh, PA, 1998
[25] C. Peng, H.B. Schlegel, Isr. J. Chem. 33 (1994) 449.
[26] C. Peng, P.Y. Ayala, H.B. Schlegel, M.J. Frisch, J. Comp. Chem. 17 (1996) 49.
[27] J.A. Pople, A.P. Scott, M.W. Wong, L. Radom, Isr. J. Chem. 33 (1993) 345.
[28] A.R.H. Cole, A.A. Green, J. Mol. Spectrosc. 48 (1973) 232.
[29] L.A. Carreira, J. Phys. Chem. 80 (1976) 1149.
[30] L.N. Margolin, Y.A. Pentin, V.I. Tyulin, Vestn. Mosk. Univ., Khim. 17 (1976) 146.
[31] G.A. Osborne, D.A. Ramsay, Can. J. Phys. 51 (1973) 1170.
[32] C.E. Blom, A. Bauder, Chem. Phys. Lett. 88 (1982) 55.
[33] G.R. De Mare, Y.N. Panchenko, A.V. Abramenkov, J. Mol. Struct. 160 (1987) 327.
[34] G.R. De Mare, Can. J. Chem. 63 (1985) 1672.
[35] T. Oie, I.A. Topol, S.K. Burt, J. Phys. Chem. 99 (1995) 905.
[36] Y. Li, T. Baer, Int. J. Mass Spectrom., in press.
[37] J.L. Holmes, J.K. Terlouw, P.C. Bergers, Org. Mass Spectrom. 15 (1980) 140.
[38] E.P. Kanter, Z. Vager, G. Both, D. Zajfman, J. Chem. Phys. 85 (1986) 7487.
[39] L.A. Curtiss, J.A. Pople, J. Chem. Phys. 88 (1988) 7405.
[40] S.G. Lias, J.E. Bartmess, J.F. Liebman, J.L. Holmes, R.D. Levin, W.G. Mallard, J. Phys. Chem. Ref. Data Vol 17, suppl. 1; NSRDS: U.S. Government Printing Office: Washington, DC, 1988.
[41] http://webbook.nist.gov/chemistry/om/, 2000.
[42] M.W. Chase, NIST-JANAF Thermochemical Tables, American Institute of Physics, New York, 1998.
[43] D.D. Wagman, W.H.E. Evans, V.B. Parker, R.H. Schum, I. Halow, S.M. Mailey, K.L. Churney, R.L. Nuttall, J. Phys. Chem. Ref. Data Vol. 11 Suppl. 2; NSRDS: U.S. Government Printing Office; Washington, 1982.
[44] W. Tsang, in: J.A. Martinho Simões, A. Greenberg, J.F. Liebman (Eds.), Energetics of Organic Free Radicals, Chapman & Hall, London, 1996, p. 22.
[45] J.C. Traeger, B.M. Kompe, in: J.A. Martinho Simões, A. Greenberg, J.F. Liebman (Eds.), Energetics of Organic Free Radicals, Chapman & Hall, London, 1996, p. 59.
[46] X. Li, H.B. Schlegel, J. Chem. Phys. 114 (2001) 8.
[47] N.L. Ma, B.J. Smith, L. Radom, Chem. Phys. Lett. 193 (1992) 386.
[48] G. Bouchoux, Y. Hoppilliard, Can. J. Chem. 60 (1982) 2107.
[49] N.L. Allinger, S. Rodriguez, K. Chen, J. Mol. Struct. (Theochem.) 260 (1992) 161.
[50] A.P. Scott, L. Radom, Int. J. Mass Spectrom. Ion Proc. 160 (1997) 73.
[51] C. Aubry, J.L. Holmes, J.K. Terlouw, J. Phys. Chem. A 101 (1997) 5958.
[52] M.T. Nguyen, H.M.T. Nguyen, Chem. Phys. Lett. 300 (1999) 346.
[53] J.C. Traeger, Org. Mass Spectrom. 20 (1985) 223.
[54] M.B. Huang, Z.X. Wang, J. Chem. Phys. 109 (1998) 8953.